ABSOLUTE CURRENT CALIBRATION OF 1μA CW ELECTRON BEAM *

M. Bevins, A. Day, P. Degtiarenko, A.P. Freyberger, A. Saha, S. Slachtouski

Jefferson Lab, Newport News, Virginia

Ronald Gilman

Rutgers University, Piscataway, New Jersey

Abstract

The future experimental program at Jefferson Lab requires an absolute current calibration of a 1 μA CW electron beam to better than 1% accuracy. This paper presents the mechanical and electrical design of a Tungsten calorimeter that is being constructed to provide an accurate measurement of the deposited energy. The energy is determined by measuring the change in temperature after beam exposure. Knowledge of the beam energy then yields number of electrons stopped by the calorimeter during the exposure. Simulations show that the energy lost due to electromagnetic and hadronic particle losses are the dominant uncertainty. Details of the precision thermometry and calibration, mechanical design, thermal simulations and simulations will be presented.

INTRODUCTION

An experiment scheduled for the Hall A end station of the Thomas Jefferson National Accelerator Facility (JLab) CEBAF accelerator requires absolute beam current measurements with 0.5% to 1.0% accuracy for beam currents around 1μA [1]. The beam current monitor is based on a pair of resonant RF cavities which need to be cross calibrated against an absolute current reference. The present absolute current calibration system is designed for currents greater then 50μA and extrapolation is required for lower beam currents [2]. In order to perform a cross calibration of the cavity response at 1μA of beam current, a new calibration device based on calorimetry is being fabricated.

The calorimeter is a slug of material that is inserted on the beam axis for a well defined period of time. The energy deposited in the calorimeter is: $E_{cal}(Joules) = E_{beam}(MeV)I_{beam}(\mu A)\Delta t(sec) - E_{loss}$ where E_{cal} is the energy absorbed by the calorimeter, E_{beam} is the energy of the beam, I_{beam} is the average beam current, Δt is the duration of the exposure and E_{loss} is the energy that escapes the slug via particle loss or thermal loss [radiation and conduction]. It is important that E_{loss} be small so that the average beam current can be extracted without additional uncertainties. The calorimeter is designed to operate with $0.8GeV < E_{beam} < 11GeV$ and $0.1\mu A < I_{beam} < 5\mu A$.

The change in temperature of the calorimeter after a

beam exposure is proportional to the energy deposited, $\Delta T = E_{cal}/\mathcal{C}_m$ where $\mathcal{C}_m$ is the specific heat of the slug. Typically heat capacities of materials are not known with the precision required for this application so $\mathcal{C}_m$ must be measured. A resistive heater inserted in the calorimeter, will be used to determine a precise value for $\mathcal{C}_m$. With nominal values of $\mathcal{C}_m$ and a 48sec exposure to a 5kW beam, the expected temperature rise is 30K.

Large copper and silver calorimeters built in the late 1960's achieved precisions of about 1% [3] and influenced the design of this calorimeter. The following sections describe the design of the calorimeter and estimates of E_{loss} and the instrumental error budget.

PARTICLE CONTAINMENT

The incident electron beam interaction in the calorimeter will result in the creation of secondary electromagnetic and hadronic particles. Electromagnetic particle/shower formation and energy leakage was studied using GEANT and EGS4 simulations. Hadronic particle formation and leakage was studied using GEANT/DINREG [5]. The optimal size, shape and material of the calorimeter from these studies is a Tungsten cylinder 16cm in diameter and 16cm long. Most of the losses are backscattered particles, and to minimize these losses the beam strikes the calorimeter within 1cm diameter by 2.5cm deep cylindrical bore. The electromagnetic loss estimate from the simulations is $0.1 \pm 0.1\%$ and the hadronic loss estimate from the simulation is $0.3 \pm 0.2\%$.

MECHANICAL DESIGN AND THERMAL CONTAINMENT

Pure tungsten shapes are typically produced by pressing and sintering tungsten powder followed by an extrusion or swaging operation to reduce porosity. Subsequent operations to reduce porosity are not practical for a part this large. An extensive search for a high thermal conductivity, high density, tungsten composite material identified a tungsten-copper (95:5) produced by OSRAM/Sylvania. This material is produced using a unique process that does not require an infiltration of copper into a sintered tungsten framework. The blended tungsten and copper powders are pressed then sintered producing a very dense (99%), homogeneous, machinable part. Copper infiltration would not be an option for a part this large.

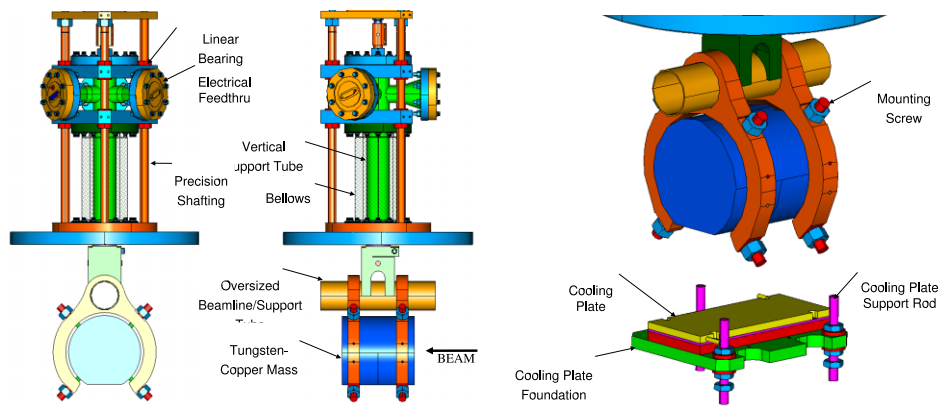Since the calorimeter must be installed upstream of the

Figure 1: Mechanical drawing the calorimeter and the support mechanism. The calorimeter and cooling plate will reside in a vacuum vessel.

physics target, the tungsten-copper mass must be inserted into the beam-line to intercept the electron beam then removed for normal beam operations to resume. A three position actuation scheme (using a three position air cylinder) minimizes actual beam time required to take a current measurement. The mass support frame incorporates an over sized beamline tube that allows beam to pass through the device in both the equilibrating and cooling positions (see figure 1). Electrical wires for thermometry, charge bleed off, and the calibration heater are routed to the mass through electrical vacuum feed-through, then down the vertical support tube, eliminating the need for a service loop inside the vacuum chamber. The electrical feed through/support tube is guided using linear ball bushings and precision shafting.

Thermal Design and Simulations   Heat leaks to and from the mass during exposure to the beam and during equilibration must be minimized, or at least known with sufficient certainty ($<<$ 1% of total absorbed energy). Socket set screws with glass ceramic inserts are used to position and support the mass inside the frame while providing thermal and electrical isolation. The mass is gold coated and the vacuum vessel electro-polished to reduce radiation exchange. The ceramic inserts used in the mounts minimize conductive heat transfer.

Advanced compliant thermal interface materials with good conductance in vacuum at low interface pressures allow the mass to be cooled for subsequent measurements by bringing it in contact with a cold plate rather than embedding or otherwise attaching cooling tubes.

Two-dimensional finite difference (FD) calculations and commercial thermal finite element (FE) [1] models were used to estimate the thermal losses, response time and temperature gradients in the calorimeter. A lumped mass model that assumes minimal spatial variation in temperature was used to estimate the time required to cool the mass to repeat a measurement. This model was used to check the results of

---

[1]The IDEAS TMG transient solver was used to build a finite element model of the calorimeter
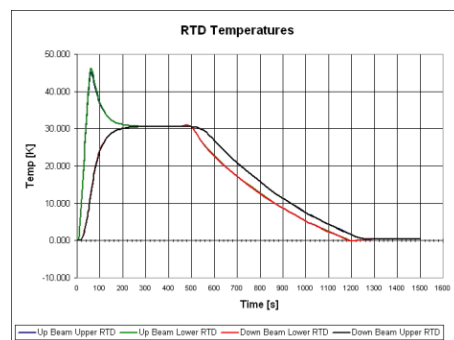

Figure 2: Thermal response of the calorimeter after a 240kJ exposure. Equilibrium is reached about 350seconds after the exposure. After 500seconds the calorimeter is lowered to the cooling plate.
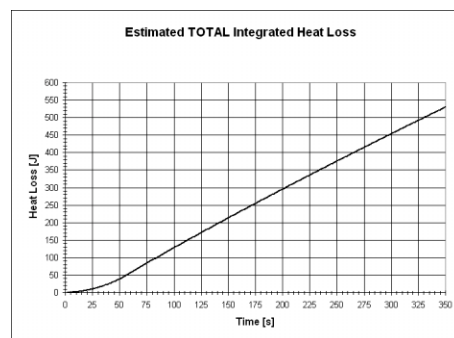

Figure 3: Estimated integrated heat loss through radiation and conduction after a deposition of 240kJ of energy in the calorimeter.

the FD code and conduct more detailed analysis that more accurately capture the transient heat flow out of (and into) the tungsten-copper mass during each of the three stages of operation (i.e., charging, equilibrating, and cooling).

The simulated thermal response of the calorimeter to 48seconds of a 5kW (240kJ) is shown in Figure 2. The calorimeter reaches equilibrium 350seconds after the expo-

sure. Figure 3 is the simulated total energy loss due to radiation and conduction through the wires and mounts. The total energy lost at 350 seconds is 530J which amounts to only 0.2% of the deposited energy. This 530J loss is dominated by radiation losses($\tilde{3}$20J), followed by the mounts ($\tilde{1}$70J) and finally the conduction loss through the instrumentation wires ($\tilde{4}$0J).

Refinements to the FE model could include radiation exchange and a model of the heater cartridge for comparisons between simulated calibration and electron beam heating. Thermal stress calculations are ongoing at this time. Preliminary conservative estimates for higher power exposures show stresses high enough to warrant more refined analysis.
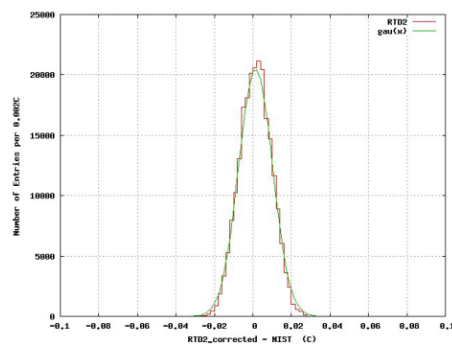
INSTRUMENTATION

Figure 4: Measured residuals for an industrial RTD after cross calibration against NIST traceable thermometer for temperature range of 20C to 60C. The data is fit to a Gaussian function with $\sigma = 0.008K$ and mean=0.002.

The absolute temperature of the calorimeter needs to measured to better than $\pm 0.025^0$K. The beam current calibration involves measuring a temperature rise,however absolute temperatures are needed for precise determination of the calorimeter's heat capacity. The heat capacity of the calorimeter is a function of temperature. Absolute temperature probes calibrated [NIST traceable] at this accuracy are expensive and bulky. Using inexpensive industrial small RTDs allows multiple and redundant temperature measurements.

The readout of the RTDs will be done by a Sensoray S518 PC104 daughter board and a PC104 CPU. The small PC104 form factor permits the readout electronics to be easily shielded and located near the calorimeter. The PC104 CPU operates Linux operated system and communicates control and monitor signals via EPICS, for ease of integration into the accelerator control system.

Calibration of the industrial RTDs against a NIST traceable thermometer has been performed by uniformly heating an Al slug of roughly the same dimension as the calorimeter and recording RTD and the NIST temperature during the decay to room temperature. The slug is suspended by thin wires in an insulated chamber [cooler]. Care must be

taken to slowly heat the slug uniformly to avoid thermal waves in the slug which result in temperature gradients. Both the RTDs and the NIST thermometer are embedded several centimeters into the slug. The default calibration constants for the industrial RTDs need to be modified by a linear correction. The typical slopes and offsets for the correction were less than 3% for the slope and 0.5K for the offset.

After calibration the RTDs measure the temperature within $\pm 0.006^0$K accuracy repeatably for several weeks of testing, see Figure 4. The tests did show that the S518 card does have a temperature dependence which must be included in the calibration constants (mainly the offset term).

SUMMARY

Table 1: Tabulation of energy losses and uncertainties for the calorimeter.

Mechanism	Loss(%)	Uncertainty(%)
Beam Energy		± 0.01
Radiation	0.13	
Conduction	0.08	
Electromagnetic particle	0.1	± 0.1
Hadronic particle	0.3	± 0.2
Instrumentation		± 0.1
Total	0.61	± 0.24

Estimated losses and uncertainties are shown in Table 1. Escaping particles represent the dominant loss and uncertainty. Thermal and mechanical design limits radiation and conduction losses to the 0.2% level. The design minimizes actual beam time required to take a measurement and allows a measurement to be repeated within 20min. The device is currently in fabrication with initial bench testing (using the heater) expected to begin summer of 2005. Installation is planned for 2006.

REFERENCES

[1] R. Gilman, "Hall A Beam Calorimeter: Overview, Specifications, Operations", JLab internal document, May 6, 2004

[2] J.-C. Denard *et.al* "High Accuracy Beam Current Monitor System For Cebaf's Experimental Hall A", Proceedings of the 2001 Particle Accelerator Conference, Chicago USA http://accelconf.web.cern.ch/AccelConf/p01/PAPERS/WPAH103.PDF

[3] G.E. Fischer and Y. Murata, "A Beam Monitor System for High-Intensity Photon Beams in the Multi-GeV Range", Nuclear Instruments and Methods, 1970

[4] P.V. Degtiarenko, "Tungsten Calorimeter Model Calculations and Radiation Issues", JLab internal document, May 14, 2004

[5] P.V.Degtyarenko and M.V.Kossov. "Monte Carlo program for nuclear fragmentation", Preprint ITEP-11, 1-18 (1992), Moscow Institute for Theoretical and Experimental Physics Preprint.